

Received: 07 August, 2024
Accepted: 16 August, 2024
Published: 17 August, 2024

*Corresponding author: Norrlaili Shapiee, Tamhidi Center, University of Islamic Sciences Malaysia, 71800 Nilai, Negeri Sembilan, Malaysia, E-mail: norrlaili@usim.edu.my

ORCID: <https://orcid.org/0000-0003-0365-3034>

Keywords: Kinetic modelling; Carbonization; Sodium carboxymethyl cellulose (CMC); Aerogels; Mass loss

Copyright License: © 2024 Shapiee N. This is an open-access article distributed under the terms of the Creative Commons Attribution License, which permits unrestricted use, distribution, and reproduction in any medium, provided the original author and source are credited.

<https://www.mathematicsgroup.us>



Research Article

Kinetic Modeling of Mass Loss during Carbonization of Sodium Carboxymethyl Cellulose (CMC) Aerogels

Norrlaili Shapiee*

Tamhidi Center, University of Islamic Sciences Malaysia, 71800 Nilai, Negeri Sembilan, Malaysia

Abstract

The carbonization of sodium carboxymethyl cellulose (CMC) aerogels involves complex thermal decomposition processes leading to the formation of carbonaceous residues. Understanding the kinetics of mass loss during carbonization is vital for optimizing the production of CMC carbon aerogels with desired properties. In this study, a mathematical model is presented that describes the kinetics of mass loss during the carbonization process of CMC aerogels. This model considers the temperature and concentration dependence of CMC decomposition reactions and is validated against experimental data obtained at various conditions. The proposed kinetic model elucidates the underlying mechanisms governing mass loss during carbonization, offering valuable insights for the design and optimization of CMC carbon aerogels across diverse applications. Furthermore, the analysis of the experimental data reveals variations in both the reaction order and the rate constant for different concentrations of CMC aerogels, indicating distinct kinetic behavior. These findings contribute to a deeper understanding of the carbonization process and pave the way for tailored synthesis approaches to meet specific application requirements.

Introduction

Aerogels are renowned for their incredibly low weight and exceptional porosity, characterized by nanopores typically ranging from 2 to 50 nanometers. These materials exhibit remarkably low thermal conductivity [1]. In the 1930s, Samuel Stephens Kistler introduced the concept of substituting the liquid phase with gas, resulting in minimal gel shrinkage, and is credited with the invention of silica aerogels [2]. Aerogels have emerged as particularly intriguing materials in the 21st century due to their remarkable characteristics, including high porosity, low density, and extensive surface area [3]. This unique architecture imparts aerogels with remarkable properties, such as high surface area, low thermal conductivity, and excellent mechanical strength relative to their weight [4]. These attributes render aerogels attractive for a wide range of applications, including insulation, lightweight structural materials, energy storage, and environmental remediation [5].

In recent years, the focus has shifted towards developing aerogels from renewable and sustainable sources to address environmental concerns and enhance their applicability [6]. Sodium carboxymethyl cellulose (CMC), a derivative of cellulose obtained from renewable biomass, has emerged as a material of growing interest [7]. CMC aerogels offer the inherent advantages of aerogels while leveraging the abundance and biodegradability of cellulose, making them an attractive option for various applications [8].

Central to the synthesis and utilization of CMC aerogels is the process of carbonization, during which CMC molecules undergo thermal decomposition to yield carbonaceous materials [9]. This transformation enhances the stability and mechanical properties of the aerogels and opens up new possibilities for tailored applications in fields such as energy storage, catalysis, and environmental remediation [10].

Understanding the kinetics of mass loss during



carbonization is essential for optimizing the production of CMC carbon aerogels with tailored properties [11]. By elucidating the underlying mechanisms governing mass loss, kinetic modelling provides valuable insights into the complex dynamics of this process, facilitating the design of optimized materials for specific applications [12].

In this context, the paper aims to develop a comprehensive kinetic model to describe the mass loss kinetics during the carbonization of CMC aerogels. By considering the temperature and concentration dependence of the decomposition reactions, this model provides a predictive tool for optimizing the synthesis of CMC carbon aerogels with desired properties.

Through a combination of experimental data and theoretical modelling, the study contributes to the fundamental understanding of the carbonization process of CMC aerogels and lays the groundwork for their efficient production and utilization across a wide range of applications.

Experimental result

In this section, the results obtained from the experimental investigation conducted on sodium carboxymethyl cellulose (CMC) aerogel are presented. The study, outlined in the paper "Preparation and Mass Loss Study of Sodium Carboxymethyl Cellulose Carbon Aerogel Prepared from Non-Hazardous Material," aimed to understand the carbonization behavior of CMC aerogel at various temperatures [13]. Carbon aerogels, with their unique properties, are recognized for their potential applications in energy storage, catalysis, and environmental remediation [14]. Understanding the mass loss behavior during carbonization is crucial for optimizing the production process and tailoring the properties of these materials to specific applications.

The experimental setup involved subjecting CMC aerogel samples to different temperatures ranging from 300°C to 800°C and monitoring the mass loss during the carbonization process. The percentage of CMC, temperature, initial and final weights of the samples, and the corresponding percentage of mass loss were recorded for each experimental run.

A detailed analysis of the experimental data is presented in this section, highlighting the trends observed in the mass loss behavior of CMC aerogel as a function of temperature. These insights contribute to a deeper understanding of the carbonization process and pave the way for further advancements in the synthesis and application of CMC-based carbon aerogels.

Based on the data presented in Table 1, it is evident that the carbonization process of CMC aerogel at various temperatures resulted in significant mass loss. The table outlines the percentage of CMC, the corresponding temperature (in °C), the weight before carbonization (WtBefore), the weight after carbonization (WtAfter), and the percentage of mass loss for each experimental run.

A consistent trend is observed across different temperatures: as the temperature increases, the percentage of mass loss

Table 1: Carbonisation of CMC aerogel at 1 hour [14].

% Of CMC	Temperature (°C)	WtBefore (g)	WtAfter (g)	% of mass loss
1	300	0.5776	0.2122	63.26
2	300	0.9211	0.4396	52.32
3	300	0.7552	0.3969	47.44
4	300	0.8795	0.4904	44.24
1	400	0.4822	0.1600	66.81
2	400	0.8135	0.3372	58.54
3	400	0.7571	0.3554	53.05
4	400	0.8588	0.4303	49.89
1	500	0.5199	0.1821	64.97
2	500	0.7149	0.3147	55.97
3	500	0.7372	0.3540	51.98
4	500	0.8347	0.4296	48.53
1	600	0.5044	0.1492	70.42
2	600	0.7323	0.2931	59.97
3	600	0.6889	0.3216	53.31
4	600	0.7794	0.3725	52.20
1	700	0.5290	0.1803	65.91
2	700	0.6624	0.2567	61.24
3	700	0.6152	0.2485	59.60
4	700	0.8614	0.3344	61.17
1	800	0.4567	0.1792	60.76
2	800	0.5602	0.3042	45.69
3	800	0.5142	0.2104	59.08
4	800	0.6579	0.2321	64.72

generally increases. For example, at 300 °C, the mass loss ranges from approximately 44.24% to 63.26%, while at 800 °C, it ranges from approximately 45.69% to 64.72%.

The increase in mass loss with higher temperatures suggests enhanced decomposition and volatilization of organic components during carbonization. Variations in mass loss percentages at the same temperature indicate that additional factors may influence the carbonization process. Potential factors include variations in the initial composition of CMC samples, differences in carbonization conditions, or heterogeneous distribution of reactants within the aerogel structure.

Overall, the results provide valuable insights into the carbonization behavior of sodium carboxymethyl cellulose (CMC) aerogel and are instrumental in further understanding its properties and applications in various fields.

Kinetic modeling APPROACH

To create a kinetic model of the mass loss during the carbonization of sodium carboxymethyl cellulose (CMC) aerogels, the experimental data provided can be used to fit various kinetic models and determine the reaction order and rate constants. One commonly used model is the kinetic model based on the nth-order reaction, also known as the power-law model [15].

The general form of the n th-order reaction model is:

$$\frac{dX}{dt} = -k(1 - X)^n$$

where:

$$\frac{dX}{dt}$$
 represents the rate of change of the extent of reaction

(X) with respect to time (t).

X is the extent of the reaction (fractional conversion of CMC).

t is time.

k is the rate constant.

n is the reaction order.

In the kinetic model for mass loss during the carbonization process, the term $(1 - X)^n$ represents the fraction of unreacted material remaining. This term is used because it reflects the decreasing amount of unreacted material over time, which influences the rate of reaction.

Definition of X : The extent of reaction (X) represents the fraction of the initial material that has undergone a reaction. Consequently, $1 - X$ represents the fraction of unreacted material remaining.

Kinetic Interpretation: In many kinetic processes, the rate of reaction is often proportional to the concentration of reactants. Here, a simplified version of the n th-order reaction model is used, where the rate of reaction is proportional to $(1 - X)^n$, indicating that the rate decreases as the fraction of unreacted material decreases.

Physical Interpretation: As the reaction proceeds, the amount of unreacted material decreases (i.e., X increases). Therefore, the rate of reaction should decrease over time. By using $(1 - X)^n$, the decrease in the rate of reaction as the reaction progresses is captured.

The expression $k(1 - X)^n$ accounts for both the rate constant (k) and the fraction of unreacted material $(1 - X)^n$ remaining, which collectively determine the rate of mass loss during carbonization. This equation describes how the extent of the reaction changes over time during the carbonization process. It represents a simplified model based on n th-order reaction kinetics, where the rate of reaction is proportional to the extent of the reaction raised to the power of the reaction order (n).

This equation can be used to model and simulate the kinetics of mass loss for different concentrations of sodium carboxymethyl cellulose (CMC) aerogels during carbonization. By fitting experimental data into this model, the reaction order (n) and the rate constant (k) for each concentration of CMC can be determined [16].

To fit the experimental data to this model, the data must

be transformed into fractional conversions and plotted against time. Subsequently, nonlinear regression can be employed to fit the data to the model and determine the reaction order (n) and the rate constant (k). By plotting the data and fitting it to the n th-order reaction model, the parameters can be obtained, allowing for a detailed discussion of the kinetic modelling of mass loss during carbonization [17].

Results and discussion

Transform the data into fractional conversions

To transform the data into fractional conversions, the extent of the reaction (X) is calculated for each data point. The extent of the reaction represents the fractional conversion of CMC and is defined as the ratio of the mass loss to the initial mass of CMC. The formula used to calculate the extent of reaction is:

$$X = \frac{m_0 - m}{m_0}$$

where:

X is the extent of reaction (fractional conversion of CMC).

m_0 is the initial mass of CMC.

m is the mass of CMC at a given time.

The extent of reaction has been calculated for each data point, and it can be plotted against time to visualize the kinetics of the carbonization process. The same calculations and data plotting can be performed using MATLAB [18].

% Experimental data

```
temperature = [300, 300, 300, 300, 400, 400, 400, 400, 500,
500, 500, 500, 600, 600, 600, 600, 700, 700, 700, 800,
800, 800, 800];
```

```
wt_before = [0.5776, 0.9221, 0.7552, 0.8795, 0.4822,
0.8135, 0.7571, 0.8588, 0.5199, 0.7149, 0.7372, 0.8347, 0.5044,
0.7323, 0.6889, 0.7794, 0.529, 0.6624, 0.6152, 0.8614, 0.4567,
0.5602, 0.5142, 0.6579];
```

```
wt_after = [0.2122, 0.4396, 0.3969, 0.4904, 0.160, 0.3372,
0.3554, 0.4303, 0.1821, 0.3147, 0.354, 0.4296, 0.1492, 0.2931,
0.3216, 0.3725, 0.1803, 0.2567, 0.2485, 0.3344, 0.1792, 0.3042,
0.2104, 0.2321];
```

```
percent_CMC = [1, 2, 3, 4, 1, 2, 3, 4, 1, 2, 3, 4, 1, 2, 3, 4, 1, 2,
3, 4, 1, 2, 3, 4];
```

% Calculate extent of reaction

```
X = (wt_before - wt_after) ./ wt_before;
```

% Set colors for each percentage of CMC

```
colors = jet(max(percent_CMC));
```

% Plot extent of reaction against temperature with % of CMC as marker color

```

figure;
for i = 1:max(percent_CMC)
    idx = percent_CMC == i;
    scatter(temperature(idx), X(idx), 50, colors(i,:), 'filled');
hold on;
end
xlabel('Temperature (°C)');
ylabel('Extent of Reaction (X)');
title('Extent of Reaction vs Temperature');
legend({'1%', '2%', '3%', '4%'}, 'Location', 'bestoutside');
grid on;
hold off;

```

Figure 1 illustrates the extent of reaction versus temperature with varying CMC concentrations. This figure provides a visual representation of how the reaction extent changes with temperature for different CMC concentrations.

In this code, the 'jet' colormap is used to assign different colors to each percentage of CMC. Each data point is marked with a color corresponding to its percentage of CMC, which allows for easy differentiation between experimental conditions.

Fitting the data to the model using nonlinear regression

To fit the experimental data to the n th-order reaction model and determine the reaction order (n) and rate constant (k), MATLAB's curve fitting toolbox or the `lsqcurvefit` function can be used for nonlinear least-squares curve fitting. The fitting can be performed using `lsqcurvefit` as follows:

```
% Define the nth-order reaction model function
```

```

nth_order_model = @(params, t) params(1) .* (params(2)
- t) .^ params(3);

```

```
% Experimental data
```

```

temperature = [300, 300, 300, 300, 400, 400, 400, 400, 500,
500, 500, 500, 600, 600, 600, 600, 700, 700, 700, 700, 800,
800, 800, 800];

```

```

wt_before = [0.5776, 0.9221, 0.7552, 0.8795, 0.4822,
0.8135, 0.7571, 0.8588, 0.5199, 0.7149, 0.7372, 0.8347, 0.5044,
0.7323, 0.6889, 0.7794, 0.529, 0.6624, 0.6152, 0.8614, 0.4567,
0.5602, 0.5142, 0.6579];

```

```

wt_after = [0.2122, 0.4396, 0.3969, 0.4904, 0.160, 0.3372,
0.3554, 0.4303, 0.1821, 0.3147, 0.354, 0.4296, 0.1492, 0.2931,
0.3216, 0.3725, 0.1803, 0.2567, 0.2485, 0.3344, 0.1792, 0.3042,
0.2104, 0.2321];

```

```

percent_CMC = [1, 2, 3, 4, 1, 2, 3, 4, 1, 2, 3, 4, 1, 2, 3, 4, 1, 2,
3, 4, 1, 2, 3, 4];

```

```
% Calculate extent of reaction
```

```
X = (wt_before - wt_after) ./ wt_before;
```

```
% Set colors for each percentage of CMC using 'jet' colormap
```

```
colors = jet(max(percent_CMC));
```

```
% Plot the experimental data with different colors for each
percentage of CMC
```

```
figure;
```

```
for i = 1:max(percent_CMC)
```

```
    idx = percent_CMC == i;
```

```
    params_fit = lsqcurvefit(nth_order_model, [1, 1, 1],
temperature(idx), X(idx));
```

```
    t_range = linspace(min(temperature(idx)),
max(temperature(idx)), 100);
```

```
    X_fit = nth_order_model(params_fit, t_range);
```

```
    plot(t_range, X_fit, 'Color', colors(i,:), 'LineWidth', 2);
```

```
hold on;
```

```
end
```

```
xlabel('Temperature (°C)');
```

```
ylabel('Extent of Reaction (X)');
```

```
title('Extent of Reaction vs Temperature');
```

```
colorbar('Ticks', linspace(0, 1, max(percent_CMC)),
'TickLabels', cellstr(num2str(1:max(percent_CMC)))));
```

```
grid on;
```

```
hold off;
```

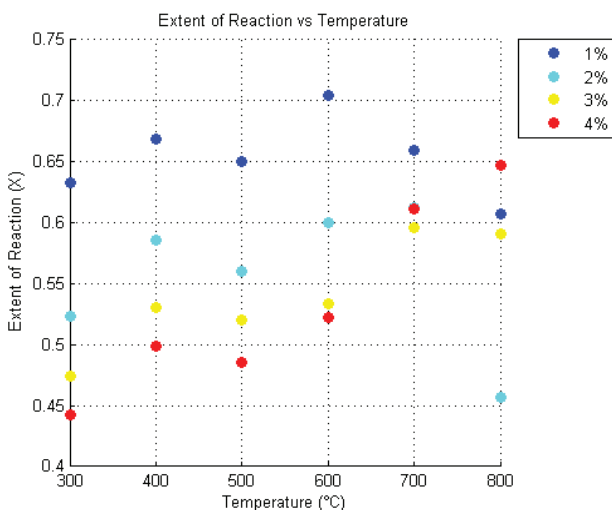


Figure 1: Extent of Reaction vs. Temperature with Varying CMC Concentrations.

Figure 2 displays the kinetics of the extent of reaction across different CMC concentrations. This figure highlights the kinetic behavior and provides insights into how the reaction kinetics vary with CMC concentration.

Analyzing Kinetic Parameters and Reaction Dynamics Across Varying CMC Concentrations

To delve into the kinetics of the carbonization process, the obtained parameter values were analyzed, providing insights into the reaction order (n), rate constant (k), and the initial extent of the reaction (X_0) across different concentrations of CMC.

```
% Define the nth-order reaction model function
nth_order_model = @(params, t) params(1) .* (params(2)
- t) .^ params(3);

% Experimental data

temperature = [300, 300, 300, 300, 400, 400, 400, 400, 500,
500, 500, 600, 600, 600, 600, 700, 700, 700, 700, 800,
800, 800, 800];

wt_before = [0.5776, 0.9221, 0.7552, 0.8795, 0.4822,
0.8135, 0.7571, 0.8588, 0.5199, 0.7149, 0.7372, 0.8347, 0.5044,
0.7323, 0.6889, 0.7794, 0.529, 0.6624, 0.6152, 0.8614, 0.4567,
0.5602, 0.5142, 0.6579];

wt_after = [0.2122, 0.4396, 0.3969, 0.4904, 0.160, 0.3372,
0.3554, 0.4303, 0.1821, 0.3147, 0.354, 0.4296, 0.1492, 0.2931,
0.3216, 0.3725, 0.1803, 0.2567, 0.2485, 0.3344, 0.1792, 0.3042,
0.2104, 0.2321];

percent_CMC = [1, 2, 3, 4, 1, 2, 3, 4, 1, 2, 3, 4, 1, 2, 3, 4, 1, 2,
3, 4, 1, 2, 3, 4];

% Calculate extent of reaction

X = (wt_before - wt_after) ./ wt_before;

% Set colors for each percentage of CMC using 'jet' colormap
```

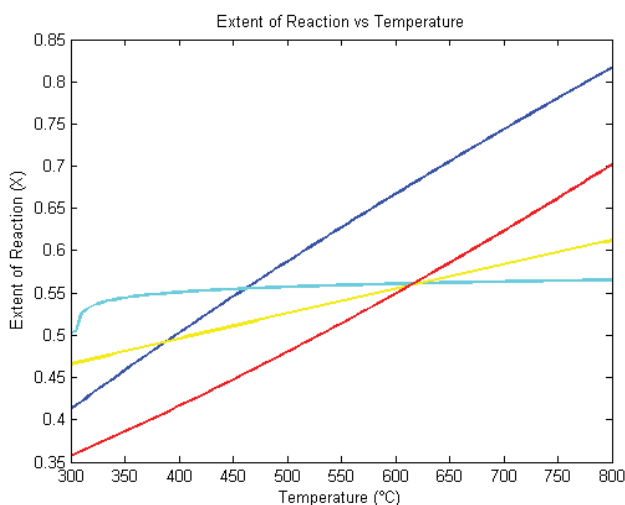


Figure 2: Extent of Reaction Kinetics across Different CMC Concentrations.

```
colors = jet(max(percent_CMC));

% Initial guess for the parameters [k, X0, n]
initial_guess = [1, 1, 1];

% Define lower and upper bounds for parameters
lb = [0, 0, 0];

ub = [Inf, Inf, Inf];

% Options for lsqcurvefit
options = optimoptions('lsqcurvefit', 'MaxFunEvals', 1000);

% Print parameter values for each percentage of CMC
for i = 1:max(percent_CMC)
    idx = percent_CMC == i;

    params_fit = lsqcurvefit(nth_order_model, initial_guess,
temperature(idx), X(idx), lb, ub, options);

    fprintf('For %d%% CMC:\n', i);

    fprintf(' k: %.2f\n', params_fit(1));

    fprintf(' X0: %.2f\n', params_fit(2));

    fprintf(' n: %.2f\n', params_fit(3));

end
```

The code is designed to print the values of k , X_0 , and n for each percentage of CMC to the MATLAB command window.

Table 2 presents the data for the carbonization of CMC aerogel at 1 hour [14]. The table includes the percentage of CMC and the corresponding values of the parameters of interest.

Kinetic Model Equations for CMC Aerogels at Various Concentrations

The given values of reaction order, n and rate constant, k for each concentration of CMC were substituted into the model equation to derive the specific kinetic model equations for 1%, 2%, 3%, and 4% CMC aerogels. (Table 3).

These equations represent the kinetic models for mass loss during the carbonization process of sodium carboxymethyl cellulose (CMC) aerogels at different concentrations. These models can be utilized to simulate and analyze the kinetics of mass loss under various conditions.

The results obtained from this study offer valuable insights into the kinetics of mass loss during the carbonization of sodium carboxymethyl cellulose (CMC) aerogels at various concentrations. The kinetic model equations derived for different concentrations of CMC demonstrate significant variation in the reaction order (n) and rate constant (k), which reflects the complexity of the carbonization process.

The observed trend of increased mass loss with higher

**Table 2:** Carbonisation of CMC aerogel at 1 hour [14].

% of CMC	<i>k</i>	<i>X</i> ₀	<i>n</i>
1	0.64	770.06	0.01
2	0.57	601.82	-0.01
3	0.04	-247.61	0.33
4	0.45	1225.66	-0.49

Table 3: Kinetic Model Equations.

% of CMC	Kinetic Model Equations
1	$\frac{dX}{dt} = 0.64(1 - X)^{0.01}$
2	$\frac{dX}{dt} = 0.57(1 - X)^{-0.01}$
3	$\frac{dX}{dt} = 0.04(1 - X)^{0.33}$
4	$\frac{dX}{dt} = 0.45(1 - X)^{-0.49}$

temperatures aligns with findings from similar studies on carbon aerogels and other porous materials [19,20]. For instance, research by Ghafoorian et al. [21] reported comparable behavior in the carbonization processes of silica aerogels, where elevated temperatures led to increased mass loss due to enhanced decomposition. Similarly, the study by Wang et al. [22] highlighted that the kinetics of mass loss for cellulose-derived aerogels exhibited significant temperature dependence, reinforcing our results.

The kinetic models developed in this study have significant implications for the optimization of carbonization processes in various applications [23]. The ability to predict mass loss behavior under different conditions can guide the design of CMC-based carbon aerogels for applications in energy storage, such as supercapacitors and batteries [24]. Additionally, the models can be used to tailor aerogels for catalytic processes and environmental remediation [25]. The ability to control and predict the carbonization process enhances the performance and efficiency of these materials in practical applications.

Several limitations should be noted in this study. First, the models are based on the assumption of *n*th-order reaction kinetics, which may not fully capture the complexity of the carbonization process. Other reaction orders or complex kinetics could be present and might require more detailed investigation. Additionally, the study focuses on a specific range of temperatures and concentrations, and the applicability of the models outside these ranges should be validated.

This work significantly advances the understanding of the carbonization process for CMC aerogels. By developing and validating kinetic models, the study provides a foundational framework for predicting and optimizing mass loss behavior. The insights gained can lead to improved design and application of CMC-based aerogels, contributing to advancements in energy storage, catalysis, and environmental remediation technologies.

In summary, this study contributes valuable knowledge to the field of aerogel carbonization. The derived kinetic models offer practical tools for simulating and optimizing the carbonization process, with implications for various high-impact applications. Future research should explore alternative kinetic models and validate the findings across a broader range of conditions to further enhance the understanding and application of CMC aerogels.

Conclusion

In this research, kinetic models were developed to describe the mass loss behaviour during the carbonization process of sodium carboxymethyl cellulose (CMC) aerogels at various concentrations. The derived kinetic models provide a mathematical framework for understanding the kinetics of mass loss during the carbonization of CMC aerogels. These models, based on *n*th-order reaction kinetics, offer valuable insights into the dependence of mass loss on reaction conditions and CMC concentration.

The analysis revealed variations in both the reaction order (*n*) and the rate constant (*k*) for different concentrations of CMC aerogels. This indicates that the kinetics of mass loss are influenced by the composition of the aerogels, with higher concentrations exhibiting distinct kinetic behaviour.

Understanding the kinetics of mass loss is crucial for optimizing the carbonization process of CMC aerogels. The developed models can aid in predicting mass loss rates under different conditions and guide the design of efficient carbonization processes for various applications.

In conclusion, the kinetic modelling study presented here enhances the understanding of mass loss behaviour during the carbonization of CMC aerogels. It lays the groundwork for further research in this area. By elucidating the kinetics of mass loss, the development of CMC-based carbon materials for applications in energy storage, catalysis, and environmental remediation can be advanced.

Acknowledgement

The author would like to extend their gratitude to all who contributed to the completion of this research.

References

- Ghaffari-Mosanenzadeh S, Tafreshi OA, Karamikamkar S, Saadatnia Z, Rad E, Meysami M, et al. Recent advances in tailoring and improving the properties of polyimide aerogels and their application. *Adv Colloid Interface Sci.* 2022;304:102646. Available from: <https://doi.org/10.1016/j.cis.2022.102646>



2. Rashid AB, Shishir SI, Mahfuz MA, Hossain MT, Hoque ME. Silica aerogel: Synthesis, characterization, applications, and recent advancements. Part Part Syst Charact. 2023;40(6):2200186. Available from: <https://doi.org/10.1002/ppsc.202200186>
3. Barrios E, Fox D, Li Sip YY, Catarata R, Calderon JE, Azim N, et al. Nanomaterials in advanced, high-performance aerogel composites: A review. Polymers. 2019;11(4):726. Available from: <https://doi.org/10.3390/polym11040726>
4. Yang M, Zhao N, Cui Y, Gao W, Zhao Q, Gao C, et al. Biomimetic architected graphene aerogel with exceptional strength and resilience. ACS Nano. 2017;11(7):6817-24. Available from: <https://doi.org/10.1021/acsnano.7b01815>
5. Peng H, Xiong W, Yang Z, Xu Z, Cao J, Jia M, et al. Advanced MOFs@ aerogel composites: construction and application towards environmental remediation. J Hazard Mater. 2022;432:128684. Available from: <https://doi.org/10.1016/j.jhazmat.2022.128684>
6. García-González CA, Budtova T, Durães L, Erkey C, Del Gaudio P, Gurikov P, et al. An opinion paper on aerogels for biomedical and environmental applications. Molecules. 2019;24(9):1815. Available from: <https://doi.org/10.3390/molecules24091815>
7. Pinto E, Aggrey WN, Boakye P, Amenuvor GA, Sokama-Neuyam YA, Fokuo MK, et al. Cellulose processing from biomass and its derivatization into carboxymethylcellulose: A review. Sci Afr. 2022;15: e01078. Available from: <https://doi.org/10.1016/j.sciaf.2021.e01078>
8. Li X, Wan C, Tao T, Chai H, Huang Q, Chai Y, et al. An overview of the development status and applications of cellulose-based functional materials. Cellulose. 2024;31(1):61-99. Available from: <https://www.springerprofessional.de/en/an-overview-of-the-development-status-and-applications-of-cellulose/26511226>
9. Ani PC, Nzereogu PU, Agbogu AC, Ezema FI, Nwanya AC. Cellulose from waste materials for electrochemical energy storage applications: A review. Appl Surf Sci Adv. 2022;11:100298. Available from: <http://dx.doi.org/10.1016/j.apsadv.2022.100298>
10. Maleki H. Recent advances in aerogels for environmental remediation applications: A review. Chem Eng J. 2016;300:98-118. Available from: <http://dx.doi.org/10.1016/j.cej.2016.04.098>
11. Konuk OP, Alsuhile AA, Yousefzadeh H, Ulker Z, Bozbag SE, García-González CA, et al. The effect of synthesis conditions and process parameters on aerogel properties. Front Chem. 2023;11:767469. Available from: <https://doi.org/10.3389/fchem.2023.1294520>
12. Lin CC, Metters AT. Hydrogels in controlled release formulations: network design and mathematical modeling. Adv Drug Deliv Rev. 2006;58(12-13):1379-1408. Available from: <https://doi.org/10.1016/j.addr.2006.09.004>
13. Atik AAA, Hassan MHA, Azhari S, Nasir NA. Preparation and mass loss study of sodium carboxymethyl cellulose carbon aerogel prepared from non-hazardous material. Malays J Sci Health Technol. 2024;10(1):1-6. Available from: <https://mjosht.usim.edu.my/index.php/mjosht/article/view/349>
14. Hu P, Tan B, Long M. Advanced nanoarchitectures of carbon aerogels for multifunctional environmental applications. Nanotechnol Rev. 2016;5(1):23-39. Available from: <https://doi.org/10.1515/ntrev-2015-0050>
15. Geng P, Zheng J, Li C, Zhang Y. Normalization of the power-law rate equation for determining the kinetic parameters of the char-CO₂ reaction. Thermochim Acta. 2021;700:178933. Available from: <https://doi.org/10.1016/j.tca.2021.178933>
16. Zhang C, Valsaraj KT, Constant WD, Roy D. Aerobic biodegradation kinetics of four anionic and nonionic surfactants at sub-and supra-critical micelle concentrations (CMCs). Water Res. 1999;33(1):115-24. Available from: [https://ui.adsabs.harvard.edu/link_gateway/1999WatRe..33..115Z/doi:10.1016/S0043-1354\(98\)00170-5](https://ui.adsabs.harvard.edu/link_gateway/1999WatRe..33..115Z/doi:10.1016/S0043-1354(98)00170-5)
17. Vyazovkin S, Burnham AK, Favregeon L, Koga N, Moukhina E, Pérez-Maqueda LA, et al. ICTAC Kinetics Committee recommendations for analysis of multi-step kinetics. Thermochim Acta. 2020;689:178597. Available from: <http://dx.doi.org/10.1016/j.tca.2020.178597>
18. Matlab S. Matlab. The MathWorks, Natick, MA, 2014;9. Available from: <https://www.mathworks.com/>.
19. Xu Z, Zhang Y, Li P, Gao C. Strong, conductive, lightweight, neat graphene aerogel fibers with aligned pores. ACS Nano. 2012;6(8):7103-13. Available from: <https://doi.org/10.1021/nn3021772>
20. Wang YY, Zhou ZH, Zhu JL, Sun WJ, Yan DX, Dai K, et al. Low-temperature carbonized carbon nanotube/cellulose aerogel for efficient microwave absorption. Compos Part B Eng. 2021;220:108985. Available from: <http://dx.doi.org/10.1016/j.compositesb.2021.108985>
21. Ghafoorian NS, Bahramian AR, Seraji MM. Investigation of the effect of rice husk derived Si/SiC on the morphology and thermal stability of carbon composite aerogels. Mater Des. 2015;86:279-88. Available from: <http://dx.doi.org/10.1016/j.matdes.2015.07.093>
22. Wan C, Jiao Y, Wei S, Zhang L, Wu Y, Li J. Functional nanocomposites from sustainable regenerated cellulose aerogels: A review. Chem Eng J. 2019;359:459-75. Available from: https://ui.adsabs.harvard.edu/link_gateway/2019ChEnJ.359..459W/doi:10.1016/j.cej.2018.11.115
23. Román S, Libra J, Berge N, Sabio E, Ro K, Li L, et al. Hydrothermal carbonization: Modeling, final properties design and applications: A review. Energies. 2018;11(1):216. Available from: <https://www.mdpi.com/1996-1073/11/1/216>
24. Gulzar U, Goriparti S, Miele E, Li T, Maidecchi G, Toma A, et al. Next-generation textiles: from embedded supercapacitors to lithium ion batteries. J Mater Chem A. 2016;4(43):16771-800. Available from: <https://pubs.rsc.org/en/content/articlelanding/2016/ta/c6ta06437j>
25. Maleki H, Hüsing N. Aerogels as promising materials for environmental remediation—a broad insight into the environmental pollutants removal through adsorption and (photo)catalytic processes. In: New polymer nanocomposites for environmental remediation. Elsevier; 2018;389-436. Available from: <https://doi.org/10.1016/B978-0-12-811033-1.00016-0>

Discover a bigger Impact and Visibility of your article publication with Peertechz Publications

Highlights

- ❖ Signatory publisher of ORCID
- ❖ Signatory Publisher of DORA (San Francisco Declaration on Research Assessment)
- ❖ Articles archived in worlds' renowned service providers such as Portico, CNKI, AGRIS, TDNet, Base (Bielefeld University Library), CrossRef, Scilit, J-Gate etc.
- ❖ Journals indexed in ICMJE, SHERPA/ROMEO, Google Scholar etc.
- ❖ OAI-PMH (Open Archives Initiative Protocol for Metadata Harvesting)
- ❖ Dedicated Editorial Board for every journal
- ❖ Accurate and rapid peer-review process
- ❖ Increased citations of published articles through promotions
- ❖ Reduced timeline for article publication

Submit your articles and experience a new surge in publication services
<https://www.peertechzpublications.org/submission>

Peertechz journals wishes everlasting success in your every endeavours.